Observation of Dispersive Shock Waves, Solitons, and Their Interactions in Viscous Fluid Conduits

Michelle D. Maiden,[1] Nicholas K. Lowman,[2] Dalton V. Anderson,[1] Marika E. Schubert,[1] and Mark A. Hoefer[1,*]

[1]*Department of Applied Mathematics, University of Colorado, Boulder, Colorado 80309, USA*
[2]*Department of Mathematics, North Carolina State University, Raleigh, North Carolina 27695, USA*
(Received 31 December 2015; revised manuscript received 10 March 2016; published 28 April 2016)

Dispersive shock waves and solitons are fundamental nonlinear excitations in dispersive media, but dispersive shock wave studies to date have been severely constrained. Here, we report on a novel dispersive hydrodynamic test bed: the effectively frictionless dynamics of interfacial waves between two high viscosity contrast, miscible, low Reynolds number Stokes fluids. This scenario is realized by injecting from below a lighter, viscous fluid into a column filled with high viscosity fluid. The injected fluid forms a deformable pipe whose diameter is proportional to the injection rate, enabling precise control over the generation of symmetric interfacial waves. Buoyancy drives nonlinear interfacial self-steepening, while normal stresses give rise to the dispersion of interfacial waves. Extremely slow mass diffusion and mass conservation imply that the interfacial waves are effectively dissipationless. This enables high fidelity observations of large amplitude dispersive shock waves in this spatially extended system, found to agree quantitatively with a nonlinear wave averaging theory. Furthermore, several highly coherent phenomena are investigated including dispersive shock wave backflow, the refraction or absorption of solitons by dispersive shock waves, and the multiphase merging of two dispersive shock waves. The complex, coherent, nonlinear mixing of dispersive shock waves and solitons observed here are universal features of dissipationless, dispersive hydrodynamic flows.

The behavior of a fluidlike, dispersive medium that exhibits negligible dissipation is spectacularly realized during the process of wave breaking that generates coherent nonlinear wave trains called dispersive shock waves (DSWs). A DSW is an expanding, oscillatory train of amplitude-ordered nonlinear waves composed of a large amplitude solitonic wave adjacent to a monotonically decreasing wave envelope that terminates with a packet of small amplitude dispersive waves. Thus, DSWs coherently encapsulate a range of fundamental, universal features of nonlinear wave systems. More broadly, DSWs occur in dispersive hydrodynamic media that exhibit three unifying features: (i) nonlinear self-steepening, (ii) wave dispersion, (iii) negligible dissipation (cf. the comprehensive DSW review article [1]).

Dispersive shock waves and solitons are ubiquitous excitations in dispersive hydrodynamics, having been observed in many environments, such as quantum shocks in quantum systems (ultracold atoms [2,3], semiconductor cavities [4], electron beams [5]), optical shocks in nonlinear photonics [6], undular bores in geophysical fluids [7,8], and collisionless shocks in rarefied plasma [9]. However, all DSW studies to date have been severely constrained by expensive laboratory setups [2,3,5,7] or challenging field studies [8], difficulties in capturing dynamical information [2,3,6], complex physical modeling [8], or a loss of coherence due to multidimensional instabilities [2,4] or dissipation [5,9]. Here, we report on a novel dispersive hydrodynamic test bed that circumvents all of these difficulties: the effective superflow of interfacial waves between

two high viscosity contrast, low Reynolds number Stokes fluids. The viscous fluid conduit system was well studied in the 1980s as a simplified model of magma transport through Earth's partially molten upper mantle [10–12] (see also the Supplemental Material [13]). This system enables high fidelity studies of large amplitude DSWs, which are found to agree quantitatively with nonlinear wave averaging or Whitham theory [22–24]. We then report the first experimental observations of highly coherent phenomena including DSW backflow, the refraction or absorption of solitons interacting with DSWs, and a multiphase DSW-DSW merger. In addition to its fundamental interest, the nonlinear mixing of mesoscopic-scale solitons and macroscopic-scale DSWs could play a major role in the initiation of decoherence and a one-dimensional, integrable turbulent state [25] that has recently been observed in optical fibers [26] and surface ocean waves [27].

In our experiment, the steady injection of an intrusive viscous fluid (dyed, diluted corn syrup) into an exterior, miscible, much more viscous fluid (pure corn syrup) leads to the formation of a stable fluid filled pipe or conduit [28]. Because of the high viscosity contrast, there is minimal drag at the conduit interface so the flow is well approximated by the Poiseulle or pipe flow relation $D \propto Q^{1/4}$, where Q is the injection rate and D is the conduit diameter. By modulating the injection rate, interfacial wave dynamics ensue. Dilation of the conduit gives rise to buoyancy induced nonlinear self-steepening regularized by normal interfacial stresses that manifest as interfacial wave dispersion [29,30]. Negligible

mass diffusion implies a sharp conduit interface and conservation of injected fluid. By identifying the azimuthally symmetric *conduit interface* as our one-dimensional dispersive hydrodynamic medium, we arrive at the counterintuitive behavior that viscous dominated, Stokes fluid dynamics exhibit dissipationless or frictionless interfacial wave dynamics. This will be made mathematically precise below.

By gradually increasing the injection rate, we are able to initiate the spontaneous emergence of interfacial wave oscillations on an otherwise smooth, slowly varying conduit. See the Supplemental Material [13] for additional experimental details. Figure 1(a) displays a typical time lapse of our experiment. At time 0 s, the conduit exhibits a relatively sharp transition between narrower and wider regions. Because of buoyancy, the fluid in the wider region moves faster than that of the narrower region. Rather than exhibit folding over upon itself, the interface begins to oscillate due to dispersive effects, as shown in Fig. 1(a) at 30 s. As later times in Fig. 1(a) attest, the oscillatory region expands, while the oscillation amplitudes maintain a regular, rank ordering from large to small. By extracting the spatial variation of the normalized conduit cross-sectional area a from a one frame per second image sequence, we display in Fig. 1(b) the full spatiotemporal interfacial dynamics as a contour plot. This plot reveals two characteristic fronts associated with the oscillatory dynamics: a large amplitude leading edge and a small amplitude, oscillatory envelope trailing edge.

We can interpret these dynamics as a DSW resulting from the physical realization of the Gurevich-Pitaevskii (GP) problem [23], a standard textbook problem for the study of DSWs [1] that has been inaccessible in other dispersive hydrodynamic systems. Here, the GP problem is the dispersive hydrodynamics of an initial jump in conduit area. Although we only have boundary control of the conduit width, our carefully prescribed injection protocol [13] enables delayed breaking far from the injection site. This allows for the isolated creation and longtime propagation of a "pure"

DSW connecting two uniform, distinct conduit areas. Related excitations in the conduit system were previously interpreted as periodic wave trains modeling mantle magma transport [11]. As we now demonstrate, the interfacial dynamics observed here exhibit a solitonlike leading edge propagating with a well-defined nonlinear phase velocity, an interior described by a modulated nonlinear traveling wave, and a harmonic wave trailing edge moving with the linear group velocity. The two distinct speeds of wave propagation in one nonlinear coherent structure are a striking realization of the double characteristic splitting from linear wave theory [22].

The long wavelength approximation of the interfacial fluid dynamics is the conduit equation [11,30]

$$a_t + (a^2)_z - [a^2(a^{-1}a_t)_z]_z = 0. \tag{1}$$

Here, $a(z,t)$ is the nondimensional cross-sectional area of the conduit as a function of the scaled vertical coordinate z and time t (subscripts denote partial derivatives). Both the interface of the experimental conduit system and Eq. (1) exhibit the essential features of frictionless, dispersive hydrodynamics: the nonlinear self-steepening (second term) due to buoyant advection of the intrusive fluid, the dispersion (third term) from normal stresses, and no dissipation due to the combination of intrusive fluid mass conservation and negligible mass diffusion [13]. The analogy to frictionless flow corresponds to the *interfacial* dynamics, not the momentum diffusion dominated flow of the bulk. The conduit equation (1) is nondimensionalized according to the cross-sectional area, vertical distance, and time in units of $A_0 = \pi R_0^2$, $L_0 = R_0/\sqrt{8\epsilon}$, and $T_0 = \mu_i/L_0 g \Delta\rho\epsilon$, respectively, where R_0 is the downstream conduit radius, $\epsilon = \mu_i/\mu_e$ is the viscosity ratio of the intrusive to the exterior liquid, $\Delta\rho = \rho_e - \rho_i$ is the density difference, and g is the gravity acceleration. Initially proposed as a simplified model for the vertical ascent of magma along narrow, viscously deformable dikes and principally used to study solitons [11,29,31], the conduit equation (1) has since been derived systematically
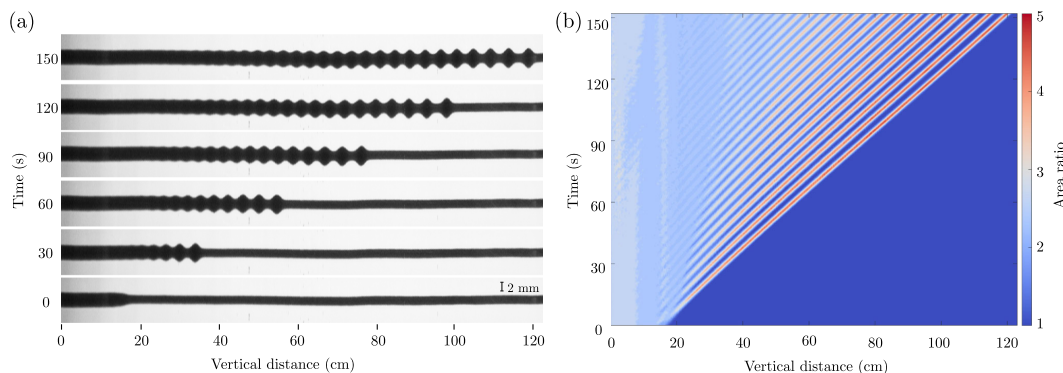

FIG. 1. Interfacial wave breaking of two Stokes fluids causing the spontaneous emergence of coherent oscillations, a DSW. The leading, downstream edge is approximately a large amplitude soliton whose phase speed is tied to the upstream conduit area. The trailing, upstream edge is a small amplitude wave packet moving at the group velocity whose wave number is tied to the downstream conduit area. (a) 90° clockwise rotated, time-lapse digital images (aspect ratio, 10:1). (b) Space-time contour plot of the conduit cross-sectional area from (a). Nominal experimental parameters, $\Delta\rho = 0.0928$ g/cm³, $\mu_i = 91.7$ cP, $\epsilon = 0.030$; downstream flow rate, $Q_0 = 0.50$ mL/min; and $a_- = 2.5$.

from the full set of coupled Navier-Stokes fluid equations using a perturbative procedure with the viscosity ratio as the small parameter [30]. The conduit equation (1) was theoretically shown to be valid for long times and large amplitudes under modest physical assumptions on the basin geometry, background velocities, fluid compositions, weak mass to momentum diffusion, and characteristic aspect ratio. The efficacy of this model has been experimentally verified in the case of solitons [29,31].

The study of DSWs involves a nonlinear wave modulation theory, commonly referred to as Whitham theory [22], which treats a DSW as an adiabatically modulated periodic wave [1,23]. Using Whitham theory and Eq. (1), key conduit DSW physical features such as the leading soliton amplitude and leading or trailing speeds have been determined [24]. For the jump in downstream to upstream area ratio a_-, Whitham theory applied to the conduit equation (1) predicts relatively simple expressions for the DSW leading s_+ and trailing s_- edge speeds,

$$s_+ = \sqrt{1 + 8a_-} - 1, \quad s_- = 3 + 3a_- - 3\sqrt{a_-(8 + a_-)},$$
$$\text{(2)}$$

in units of the characteristic speed $U_0 = L_0/T_0$. The leading edge approximately corresponds to an isolated soliton where the modulated periodic wave exhibits a zero wave number. Given the speed s_+, the soliton amplitude a_+ is implicitly determined from the soliton dispersion relation $s_+ = [a_+^2(2 \ln a_+ - 1) + 1]/(a_+ - 1)^2$ [29]. At the trailing edge, the modulated wave limits to zero amplitude, corresponding to harmonic waves propagating with the group velocity $s_- = \omega'(k_-)$, where $\omega(k) = 2a_-k/(1 + a_-k^2)$ is the linear dispersion relation of Eq. (1) on a background conduit area a_- and $k_-^2 = [a_- - 4 + \sqrt{a_-(8 + a_-)}]/(4a_-)$ is the distinguished wave number determined from modulation theory [24] (see also Ref. [1]).

In Fig. 2, we compare the leading edge amplitude and speed predictions with the experiment, demonstrating quantitative agreement for a range of jump values a_-. The analytical theory (Whitham theory) is known to break down at large amplitudes [24], so we also include direct determination of the speed and the amplitude from numerical simulation of Eq. (1), demonstrating even better agreement. In order to obtain the reported dimensionless speeds of Fig. 2(a), we divide the measured speeds by U_0 with μ_i determined by fitting the downstream conduit area to a Poiseulle flow relation. This enables us to self-consistently account for the shear-thinning properties of corn syrup. All the remaining fluid parameters take their nominal, measured values. The deviation between experiment and theory at large jump values is consistent with previous measurements of solitons, where the soliton dispersion relation was found to underpredict observed speeds at large amplitudes [29] (see also the Supplemental Material [13]).

In addition to single DSWs, our experimental setup allows us to investigate exotic, coherent effects predicted
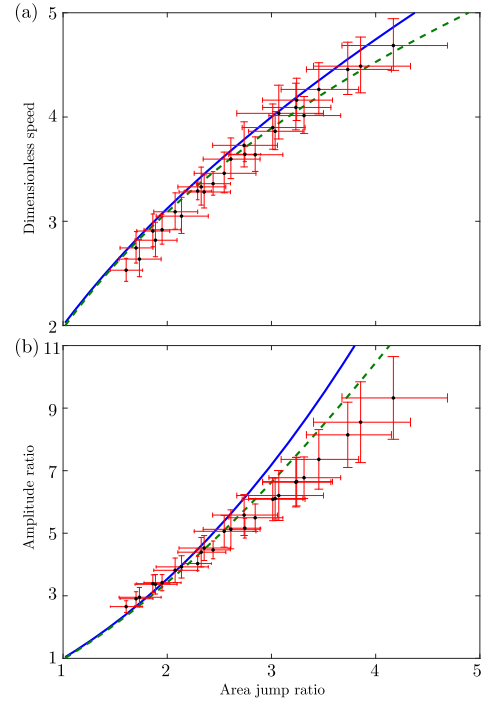

FIG. 2. Comparison of observed and predicted leading edge DSW amplitude and speed. Observations (circles), Whitham modulation theory (solid curves), and numerical simulation of the conduit equation (dashed curves) for (a) DSW leading edge speeds s_+ and (b) DSW leading amplitude a_+ versus downstream area ratio a_-. Nominal experimental parameters, $\Delta\rho = 0.1305$ g/cm^3 $\mu_i = 80.4$ cP (measured), $\mu_i = 104$ cP (fitted), $\epsilon = 0.0024$. See the Supplemental Material [13] for the fitting procedure.

by Eq. (1) for the first time. For example, backflow is a feature of dispersive hydrodynamic systems whereby a portion of the DSW envelope propagates upstream. This feature occurs here when the group velocity of the trailing edge wave packet is negative. From the expression for s_- in Eq. (2), we predict the onset of backflow when a_- exceeds $8/3$. In Fig. 3, we utilize our injection protocol to report the observation of this phenomenon in the viscous conduit setting (see the Supplemental Material [13] for videos). Waves with a strictly positive phase velocity are continually generated at the trailing edge, but the envelope group velocity is negative. We estimate the crossover to backflow for the experiments reported in Fig. 2 at $a_- \approx 3$, consistent with a slightly larger crossover than theory ($8/3$) due to the subimaging resolution of small amplitude waves.

The ease with which DSWs and solitons can be created in this viscous liquid conduit system enables the investigation of novel coherent, nonlinear wave interactions. In Fig. 4, we report soliton-DSW and DSW-DSW interactions from our conduit experiment (see the Supplemental Material [13] for videos). As in previous experiments [29,31], an isolated conduit soliton is created by the pulsed injection of fluid on top of the steady injection that maintains the background conduit. Figures 4(a) and 4(b) depict the generation of a DSW
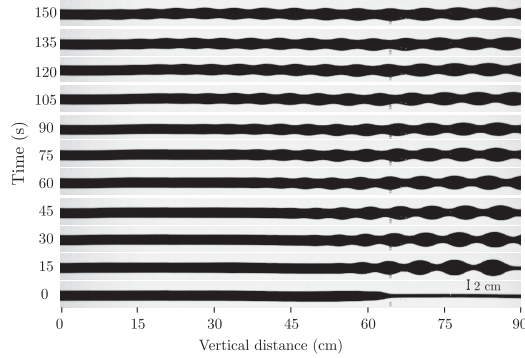
FIG. 3. Time-lapse images (aspect ratio, 1:1) of large amplitude wave breaking leading to an upstream propagation of the DSW trailing edge envelope: DSW backflow. Nominal experimental parameters, $\Delta\rho = 0.0983$ g/cm^3, $\mu_i = 93.5$ cP, $\epsilon = 0.029$, $a_- = 4$, and $Q_0 = 0.50$ mL/min.

followed by a soliton. Because solitons propagate with a nonlinear phase velocity larger than the linear wave phase and group velocities [29], the soliton eventually overtakes the DSW trailing edge. The soliton-DSW interaction results in a sequence of phase shifts between the soliton and the crests of the modulated wave train. The soliton emerges from the interaction with a significantly increased amplitude and decreased speed due to the smaller downstream conduit upon which it is propagating. The initial and final slopes of

soliton propagation in Fig. 4(b) demonstrate that the soliton has been refracted by the DSW. Meanwhile, the DSW experiences a subtle phase shift and is otherwise unchanged.

The opposite problem of a soliton being overtaken by a DSW is displayed in Fig. 4(c). After multiple phase shifts during interaction, the soliton is slowed down and effectively absorbed within the interior of the DSW, while the DSW is apparently unchanged except for a phase shift in its leading portion. Such behavior is consistent with the interpretation of a DSW as a modulated wave train with small amplitude trailing waves that will always move slower than a finite amplitude soliton.

Figure 4(d) reveals the interaction of two DSWs. The interaction region results in a series of phase shifts similar to soliton-soliton interactions that form a quasiperiodic or two-phase wave train, as shown in the inset. This nonlinear mixing eventually subsides, leaving a single DSW representing the merger of the original two. The trailing DSW has effectively been refracted by the leading DSW.

We can interpret the soliton and DSW refraction as follows. First, consider the overtaking interaction of two DSWs. Denote the midstream and upstream conduit areas $a_1 < a_2$ relative to the downstream area $a_0 = 1$. Equation (2) implies that the leading edge speeds of the first and second DSWs are $s_1 = \sqrt{1 + 8a_1} - 1$, $s_2 = a_1(\sqrt{9 + 8(a_2 - 1)/a_1} - 1)$. Motivated by previous DSW interaction studies [32], we
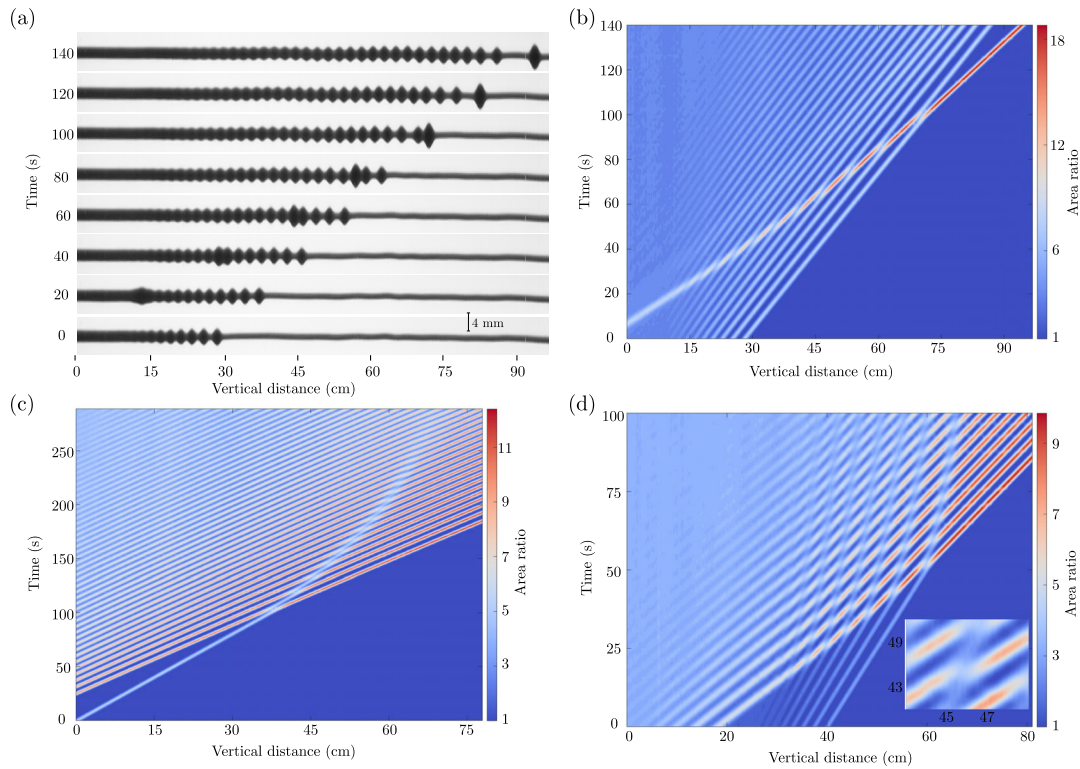

FIG. 4. Interactions of solitons and DSWs. Time-lapse images with (a) the aspect ratio 10:1 and (b) the space-time contour of DSW-soliton interaction revealing soliton refraction by a DSW with $a_- = 3$. (c) Space-time contour of the absorption of a soliton by a DSW with $a_- = 3.5$. (d) DSW-DSW interaction and merger causing the multiphase mixing (inset) and the refraction of the trailing DSW by the leading DSW with $a_1 = 2.5$, $a_2 = 5$. Nominal experimental parameters, $\Delta\rho = 0.0971$ g/cm^3, $\mu_i = 99.1$ cP, $\epsilon = 0.029$, $Q_0 = 0.2$ mL/min.

assume the merger of the two DSWs and thus obtain the leading edge speed of the merged DSW $s_m = 4\sqrt{\frac{1}{2}(a_1 + a_2) - 1} - 1$ connecting the conduit area a_0 to a_2. One can verify the interleaving property $s_1 < s_m < s_2$, demonstrating the refraction (slowing down) of the second DSW. If we treat the isolated soliton as the leading edge of a DSW, then we obtain the same result for soliton-DSW refraction.

Viscous liquid conduits are a model system for the coherent dynamics of one-dimensional superfluidlike media with microscopic-scale fluid dynamics [12], mesoscopic-scale solitons [31], and macroscopic-scale DSWs as fundamental nonlinear excitations. Interactions of DSWs and solitons suggest that soliton refraction, absorption, multiphase dynamics, and DSW merging are general, universal features of dispersive hydrodynamics. The viscous liquid conduit system is a new environment in which to investigate complex, coherent dispersive hydrodynamics that have been inaccessible in other superfluidlike media.

---

*hoefer@colorado.edu

[1] G. A. El and M. A. Hoefer, arXiv:1602.06163 [Physica D (Amsterdam) (to be published)].

[2] Z. Dutton *et al.*, Science **293**, 663 (2001); J. J. Chang, P. Engels, and M. A. Hoefer, Phys. Rev. Lett. **101**, 170404 (2008).

[3] M. A. HoeferM. A. Hoefer, M. J. Ablowitz, I. Coddington, E. A. Cornell, P. Engels, and V. Schweikhard, Phys. Rev. A **74**, 023623 (2006); M. A. Hoefer, P. Engels, and J. Chang, Physica D (Amsterdam) **238**, 1311 (2009); R. Meppelink, S. B. Koller, J. M. Vogels, P. van der Straten, E. D. van Ooijen, N. R. Heckenberg, H. Rubinsztein-Dunlop, S. A. Haine, and M. J. Davis, Phys. Rev. A **80**, 043606 (2009); J. A. Joseph, J. E. Thomas, M. Kulkarni, and A. G. Abanov, Phys. Rev. Lett. **106**, 150401 (2011).

[4] A. Amo *et al.*, Science **332**, 1167 (2011).

[5] Y. C. Mo, R. A. Kishek, D. Feldman, I. Haber, B. Beaudoin, P. G. O'Shea, and J. C. T. Thangaraj, Phys. Rev. Lett. **110**, 084802 (2013).

[6] J. E. Rothenberg and D. Grischkowsky, Phys. Rev. Lett. **62**, 531 (1989); W. Wan, S. Jia, and J. W. Fleischer, Nat. Phys. **3**, 46 (2007); S. Jia, W. Wan, and J. W. Fleischer, Phys. Rev. Lett. **99**, 223901 (2007); C. Barsi, W. Wan, C. Sun, and J. W. Fleischer, Opt. Lett. **32**, 2930 (2007); C. Conti, A. Fratalocchi, M. Peccianti, G. Ruocco, and S. Trillo, Phys. Rev. Lett. **102**, 083902 (2009); N. Ghofraniha, L. S. Amato, V. Folli, S. Trillo, E. DelRe, and C. Conti, Opt. Lett. **37**,

2325 (2012); J. Fatome, C. Finot, G. Millot, A. Armaroli, and S. Trillo, Phys. Rev. X **4**, 021022 (2014).

[7] J. L. Hammack and H. Segur, J. Fluid Mech. **84**, 337 (1978); S. Trillo, M. Klein, G. F. Clauss, and M. Onorato, Physica D (Amsterdam), doi:10.1016/j.physd.2016.01.007 (in press).

[8] D. Farmer and L. Armi, Science **283**, 188 (1999); A. Porter and N. F. Smyth, J. Fluid Mech. **454**, 1 (2002); C. R. Jackson, Global Ocean Associates, 2004, http://www.internalwaveatlas.com/Atlas2_index.html; A. Scotti, R. C. Beardsley, B. Butman, and J. Pineda, J. Geophys. Res. **113**, C08031 (2008).

[9] R. J. Taylor, D. R. Baker, and H. Ikezi, Phys. Rev. Lett. **24**, 206 (1970); M. Q. Tran, K. Appert, C. Hollenstein, R. W Means, and J. Vaclavik, Plasma Phys. **19**, 381 (1977).

[10] D. R. Scott and D. J. Stevenson, Geophys. Res. Lett. **11**, 1161 (1984).

[11] D. R. Scott, D. J. Stevenson, and J. A. Whitehead, Nature (London) **319**, 759 (1986).

[12] J. A. Whitehead and K. R. Helfrich, Nature (London) **336**, 59 (1988).

[13] See Supplemental Material at http://link.aps.org/supplemental/10.1103/PhysRevLett.116.174501, which includes Refs. [14–21], for additional experimental details, videos corresponding to each figure, and historical background material on viscous fluid conduits.

[14] D. McKenzie, J. Petrol. **25**, 713 (1984).

[15] J. A. Whitehead, K. R. Helfrich, and M. P. Ryan, *Magma Transport and Storage* (Wiley, Chichester, England, 1990).

[16] G. Simpson and M. I. Weinstein, SIAM J. Math. Anal. **40**, 1337 (2008).

[17] C. Wiggins and M. Spiegelman, Geophys. Res. Lett. **22**, 1289 (1995).

[18] M. Spiegelman, J. Fluid Mech. **247**, 39 (1993).

[19] T. Elperin, N. Kleeorin, and A. Krylov, Physica D (Amsterdam) **74**, 372 (1994).

[20] T. R. Marchant and N. F. Smyth, IMA J. Appl. Math. **70**, 796 (2005).

[21] E. Ray, P. Bunton, and J. A. Pojman, Am. J. Phys. **75**, 903 (2007).

[22] G. B. Whitham, *Linear and Nonlinear Waves* (Wiley, New York, 1974).

[23] A. V. Gurevich and L. P. Pitaevskii, Sov. Phys. JETP **38**, 291 (1974).

[24] N. K. Lowman and M. A. Hoefer, J. Fluid Mech. **718**, 524 (2013).

[25] G. A. El and A. M. Kamchatnov, Phys. Rev. Lett. **95**, 204101 (2005).

[26] S. Randoux, P. Walczak, M. Onorato, and P. Suret, Phys. Rev. Lett. **113**, 113902 (2014).

[27] A. Costa, A. R. Osborne, D. T. Resio, S. Alessio, E. Chrivì, E. Saggese, K. Bellomo, and C. E. Long, Phys. Rev. Lett. **113**, 108501 (2014).

[28] J. A. Whitehead, Jr. and D. S. Luther, J. Geophys. Res. **80**, 705 (1975).

[29] P. Olson and U. Christensen, J. Geophys. Res. **91**, 6367 (1986).

[30] N. K. Lowman and M. A. Hoefer, Phys. Rev. E **88**, 023016 (2013).

[31] K. R. Helfrich and J. A. Whitehead, Geophys. Astrophys. Fluid Dyn. **51**, 35 (1990); N. Lowman, M. Hoefer, and G. El, J. Fluid Mech. **750**, 372 (2014).

[32] M. J. Ablowitz, D. E. Baldwin, and M. A. Hoefer, Phys. Rev. E **80**, 016603 (2009); M. J. Ablowitz and D. E. Baldwin, Phys. Rev. E **87**, 022906 (2013).